

Hygrothermal Influence of Air Convection in Wall Structures

T. Ojanen

R. Kohonen, Ph.D.

ABSTRACT

A numerical simulation model, TOCC2D (Transient Coupled Convection and Conduction in 2-Dimensions), to analyze the transient hygrothermal behavior of porous, multilayer building structures with coupled convection and conduction in two dimensions has been developed. In the paper, the influence of air convection on the hygrothermal performance of wall structures based on calculations with TOCC2D, and laboratory and field experiments will be discussed.

According to measurements, natural convection may increase heat losses through a lightweight mineral fiber wall structure by 10% or more. The calculated value for an ideal, closed structure is no more than 1%. This difference is mostly due to the non-idealities of a real multilayer structure. The structural airtightness is one of the main parameters affecting the hygrothermal behavior of building structures.

The wind-caused forced convection may increase heat losses of a wall structure, especially in corners. The effects of convection vary case by case due to air permeances of the structures. Compared to a pure heat conduction case, even a moderate wind may, according to measurements, increase the mean heat losses of the corner area by about 15%. In this case, the calculated heat flux values were locally even three times higher than without convection.

Air infiltration and exfiltration causes heat recovery from transmission heat losses. In the case with uniform air infiltration ($0.5 \text{ dm}^3/\text{s}\cdot\text{m}^2$) through 100-mm-thick mineral fiber insulation structure, the calculated warming of the air is about 90%. Total heat recovery effect, considering the heat balance of the room air, is, in this case, about 23%. Heat recovery effect has a maximum value, which depends on the air infiltration rate and the thermal resistance of the structure. When the infiltrating airflow rate exceeds this optimum value, the heat losses of the wall are almost equal to those of a wall with lower thermal resistance, i.e., the same thermal performance could be achieved with thinner thermal insulation.

Air exfiltration probably will take place for short terms locally because of the varying air pressure conditions. Long-time inside airflow through a structure may cause severe moisture damages. Influence of air exfiltration on moisture conditions will be illustrated by some typical cases. Limits for critical exfiltration rates should be analyzed case by case because they depend both on the hygrothermal properties of the structure and the inside air and climate conditions.

INTRODUCTION

Air convection in wall structures may considerably change the hygrothermal performance of a structure from that of the non-convective case. Convection may take place as a flow in macro-porous building materials or only locally as a crack flow in material joints. It is

R. Kohonen, Leading Research Scientist, Technical Research Centre of Finland, and T. Ojanen, Research Scientist, Technical Research Centre of Finland

caused by gravitational, temperature-difference-dependent buoyancy, outside pressure gradient (wind) or pressure differences between inside and outside air spaces. The airflow velocity and direction may vary strongly due to the changing boundary conditions.

This paper presents results of numerical simulation on convection in wall structures. The cases are chosen so that a view from both the thermal behavior and the moisture movements and possible accumulation in structures due to air convection could be provided. The simulation model TCCC2D, which was used in the analysis, has been verified with several laboratory and field experiments (Kohonen et al. 1985, 1986). One aim of the study was to get a better understanding of the critical conditions for convection-caused heat and moisture flow in typical, lightweight wall structures.

TYPICAL CASES OF AIR CONVECTION IN BUILDING STRUCTURES

Convection can be separated into natural and forced convection, which may be present both separately or at the same time. Figure 1 presents some flow fields, which are typical for lightweight wall structures. In Case A the structure is closed, which means that both the inside covering board and the wind barrier are airtight compared with the (fibrous) thermal insulation, so a closed convection loop is formed by natural convection only. In Case B the air permeance of the wind barrier is rather low, and the airflow through the outside surface of the structure is dominating. Also, forced convection may contribute to the airflow.

Case C illustrates a typical forced convection flow between an air space and the wall structure, for example, when the wind causes pressure differences over a corner. In Cases D through F the air flows through the whole structure from one air space to another, the pressure conditions of which usually differ from each other. Infiltration/exfiltration airflow can be caused by temperature difference only, but pressure differences between inside and outside air spaces are usually more significant.

Natural convection is caused by air density differences. The driving force of natural convection is with a maximum temperature difference usually only about 1/10 or less than that of wind-caused air pressure difference. However, natural convection has a considerable influence on the temperature field of a wall structure like Figure 2, which shows test setup of laboratory experiments and the measured heat flux distribution for structures with pure natural convection (types A and B in Figure 1). Without convection the heat flux should be constant throughout the structure height, but the heat flux varies from 2 to 10 W/K·m² due to natural convection. Although the wall structures were assembled in laboratory conditions, similar structures had quite different heat flux distributions with the same boundary conditions. These results also show that in typical structures with wood framing and mineral fiber thermal insulation, there are likely non-idealities, which strongly affect the thermal performance of structures.

Forced convection (Case C in Figure 1) occurs mostly in corner areas and structural joints, where the structural thermal bridges, combined with convection, may locally increase the U-value of a structure from that of the ideal case.

Strong, local air leakage through a structure may essentially reduce the thermal resistance of the wall structure and also the thermal comfort of the indoor space by lowering surface temperatures and increasing cold airflow in the room space. However, if the infiltrating air is uniformly distributed in thermal insulation, the heat recovery from transmission heat losses warming up the incoming air may significantly reduce the total heat losses of the room space.

This paper also emphasizes the numerical study of a dynamic insulation structure, which includes analysis of the potential effects of the heat recovery and risks for moisture accumulation with different structures and varying airflow rates and directions.

NUMERICAL SIMULATION

It is often difficult to experimentally determine the effects of a certain parameter on the hygrothermal performance of a structure. The number as well as the duration of the experiments is limited and, for example, the non-idealities of the structures affect the measured results.

Numerical simulation makes it possible to study separately the effects of different structural parameters and boundary conditions. Calculations can be made with exactly known parameter values, which experimentally would often be nearly impossible. Experimental research is important for verification of calculation models and also for analyzing more thoroughly those cases that are found to be most interesting in numerical simulation.

Numerical Simulation Model TCCC2D

TCCC2D (Transient Coupled Convection and Conduction in 2-Dimensions) solves the two-dimensional heat and moisture flow in multilayer building structures. Pressure, temperature, and partial vapor pressure are used as driving potentials. The Darcy flow equation with Boussinesq approximation for incompressible fluid is used. Local thermodynamic equilibrium is assumed between stagnant and flowing phases. Phase changes may, however, occur.

The continuity, momentum, energy, and mass balance equations can be given in component form with Equations 1 through 4:

Mass balance:

$$\frac{\partial \rho_f}{\partial t} + \frac{\partial (\rho v_x)}{\partial x} + \frac{\partial (\rho v_y)}{\partial y} = 0 \quad (1)$$

Momentum:

$$v_{x,f} = -K_{v,x}/\eta_f \frac{\partial p_f}{\partial x} \quad (2 a)$$

$$v_{y,f} = -K_{v,y}/\eta_f \left(\frac{\partial p_f}{\partial y} - \rho_f g \right) \quad (2 b)$$

Energy balance:

$$c'' \frac{\partial T}{\partial t} = \frac{\partial}{\partial x} \left(\lambda_x \frac{\partial T}{\partial x} \right) + \frac{\partial}{\partial y} \left(\lambda_y \frac{\partial T}{\partial y} \right) \quad (3)$$

$$- \frac{\partial}{\partial x} (\rho c_p v_x T)_f - \frac{\partial}{\partial y} (\rho c_p v_y T)_f$$

Moisture balance:

$$\frac{\partial (u \rho_0)}{\partial t} = \frac{\partial}{\partial x} \left(\lambda_{D,x} \frac{\partial p_h}{\partial x} \right) + \frac{\partial}{\partial y} \left(\lambda_{D,y} \frac{\partial p_h}{\partial y} \right) \quad (4)$$

$$- \frac{\partial}{\partial x} (\rho_h v_x) - \frac{\partial}{\partial y} (\rho_h v_y)$$

An ordinary finite-difference method is used in the numerical solution. Variables are calculated at the grid points, while flows are calculated at the mid-point of grids. For the time derivative, the Crank-Nicholson approach is used. Moisture content of each material is coupled with partial vapor pressure and temperature by sorption isotherms. Figure 3 presents the coupling between pressure, temperature, and moisture fields.

TCCC2D is used on a mainframe computer, but a PC version has also been developed, which runs under DOS 3.30, though the size of the network for the structure is more limited.

Natural Convection

In the following, the Nusselt number, Nu, describes the ratio between the total heat flow under convection and that without convection for a certain control surface of a wall structure. If the Nusselt number >1, then convection has increased the average heat flow from the non-convective case.

Figure 4 shows how the Nusselt number for closed and semiopen (Figure 1, a and b) structures depends on the modified Rayleigh number, Ra* (Equation 5), and the aspect ratio, i.e., the ratio between structure height h and thickness d. In these cases the maximum value for the Nusselt number is reached with the aspect ratio of the order of 1.5. The ratio of air permeabilities in vertical and horizontal directions of the mineral fiber insulation material was also 1.5.

$$Ra^* = g \beta \left(\frac{\rho \cdot c_p}{\nu} \right) \frac{4 K_{v,x} K_{v,y}}{F \left((\lambda_y K_{v,x})^{1/2} + (\lambda_x K_{v,y})^{1/2} \right)^2} \Delta T d \quad (5)$$

The calculated value for the Nusselt number is significantly higher for semi-open structures than for closed structures. With Ra* = 5.2, the closed structure had a Nu value of 1.006 but the Nu value for the semiopen structure with the same Ra* value was 1.08.

In measurements with 2.2 m high and 300 mm thick fiberglass insulation (17 kg/m³) (Kohonen et al. 1986), the heat flux distribution had no clear dependence on the structure type, as Figure 2 shows. Figure 2 illustrates the case with the weakest correspondence to the predicted results. The measured Nusselt numbers for closed structures were about 1.1 to 1.15. The differences between measured and calculated values are due to the non-idealities of the real structures. According to measurements, it is obvious that a numerical simulation model cannot solve the exact airflow and temperature field of a real structure because of the non-predictable leakage routes.

Figure 5 shows how the calculated ideal case differs from the measured one in a case with 2.2 m high, 300 mm thick (19 kg/m³) mineral fiber thermal insulation with ΔT=40 K. The temperature difference between measured and calculated values for ideal structures varied about from 0°C to 7°C. When assuming small air cracks (described by locally higher permeability values) for material joints, the difference was still about 3°C in one point, but the shape of the calculated temperature fields of semiopen structures matched much better with the measured ones.

The more material joints there are in a structure the more these joints contribute to convection by forming local airflow routes, which cannot be considered accurately in numerical simulation. Calculations on ideal structures give the minimum limit for the influence of convection, which can be considered as a reference for the hygrothermal behavior of a structure.

Figure 4 shows how the Nusselt number increases when the aspect ratio decreases from typical values for wall structures. In Figure 6 the effects of horizontal convection obstructions for the vertical heat flux distribution of a structure are presented. In the calculations, a horizontal airtight plate was placed in the middle of a 2.2-m-high, 0.3-m-thick mineral-fiber-insulated structure that had an open cold surface. Temperatures of the inside and outside air spaces were +20 and -20°C, respectively. The modified Rayleigh number was 5.2.

If the thermal resistance of the convection obstruction is relatively high, then it divides the wall into two separate parts (aspect ratio from 7.33 to about 3.6 each), and so the Nusselt number increases from 1.08 to 1.10. But if the convection obstruction has no thermal resistance, then the Nusselt number decreases to 1.05 because of the heat recovery effect between the warm air leaving the lower part of the wall and the cold air flowing into the upper part of the divided structure.

Vertical convection obstructions seem to be even more efficient in reducing convection. If a vertical convection obstruction is placed inside the thermal insulation, the aspect ratio increases, which will reduce the Nusselt number. Vertical obstructions inside a structure may, however, cause severe problems by affecting moisture flow and the normal drying of the wall.

Forced Convection

Wind causes pressure differences between different parts of the building envelope. The pressure gradients and airflow velocities are usually highest near structural joints, for example, in corners and in wall and ceiling joints. The correlation between wind velocity and structural pressure gradient is dependent on the wind damping of the structure, air permeance of the wind barrier and other structural means of reducing wind effects and also on the workmanship. For example, in field experiments with typical lightweight building envelopes, about 60 Pa hourly mean values for pressure differences have been measured over corner areas with the wind speed of 9 m/s (Kohonen et al. 1986).

The thermal influence of forced convection was studied in field experiments with a structure with airtight inside covering, 190 mm mineral fiber insulation (20 kg/m^3), and a 50 mm mineral fiber wind barrier, which was bounded by a 20 mm air gap open to outside air. Air permeabilities of the thermal insulation and wind barrier were $K_v = 2.5 \cdot 10^{-9} \text{ m}^2$ and $0.4 \cdot 10^{-9} \text{ m}^2$, respectively.

Figure 7 illustrates the structure and the measured and calculated relative temperature values at the boundary of the thermal insulation and the wind barrier ($x = 50$ and $y = 1750 \text{ mm}$) and in the middle of the thermal insulation ($x = 145$ and $y = 1655 \text{ mm}$), when the pressure difference over the corner area is 27 and 63 Pa.

The shape of the calculated temperature distribution corresponded relatively well to the measured values, although in the middle of the thermal insulation the calculated values reached the outside temperature value, while the measured minimum value of the relative temperature was about 0.1. Because of the structural thermal bridge and strong airflow (the direction of which changes due to the wood framing and other material layers) the heat flux values change sharply at the corner area (Figure 8). In Figure 8, the calculated heat fluxes for a structure with $\Delta T = 10^\circ\text{C}$ are presented as well as the inside surface temperatures with $\Delta T = 40^\circ\text{C}$.

Calculations were also done assuming a structure without wood framing. In this case, convection increases and, while the direction of airflow does not change before the corner, which would damp the influence of the cold airflow, heat losses in the corner area increase. The local maximum heat flux could even be two times higher than in the normal case with wood framing.

If the outside air is cold, a strong convection flow can reduce the inside surface temperatures and thus affect the thermal comfort of the room space or even cause water vapor condensation. The calculated inside surface temperatures of the mineral fiber insulation for the structure in Figure 7 are also given in Figure 8. The inside and outside temperatures are $+20$ and -20°C , respectively, and the pressure difference is $\Delta p = 63 \text{ Pa}$. An ideal structure will have a local minimum surface temperature value of $+10^\circ\text{C}$ just after the airflow has passed the wood framing in the corner. Without any internal flow obstruction, the local minimum value for surface temperature would be as low as $+1^\circ\text{C}$, which would cause surface condensation.

According to the results, the thermal performance of a building envelope may differ distinctively in the corner areas from that of a separate wall without any hydraulic connection to the adjoining structures. Airflow routes in corner areas and the non-idealities (air cracks, etc.), which are likely to appear in structural joints, may increase convection locally. Thus the structural means to reduce local air pressure gradients would permit a correct thermal performance for the whole building envelope when considering the effects of forced convection.

Air Infiltration / Exfiltration

In many cases outdoor air flows into the room space totally or at least partly through the building envelope via air inlets and structural air leakage routes. During the heating period, when the outside air temperature is low, the influence of the infiltrating air on the temperature field of the leaky parts of the structure may be drastic.

When the air infiltrates through the building envelope, the heat recovery from transmission heat losses warms up the incoming air and the total heat losses reduce from those without any heat recovery. The efficient use of a dynamic wall structure requires that the airflow be uniformly distributed over the structure.

In order to analyze the potential effects of heat recovery with air infiltration, convection Cases D through F (Figure 1) were analyzed. The presented calculations analyzed a structure with uniformly distributed airflow (D). The structure was assembled of mineral fiber thermal insulation ($\lambda = 0.034 \text{ W/K}\cdot\text{m}$, 20 kg/m^3), with different thicknesses (100, 150, and 200 mm) and a 12 mm covering board ($\lambda = 0.055 \text{ W/K}\cdot\text{m}$) at the inside surface of the structure. Because only the thermal effects of dynamic walls were analyzed as a function of airflow rate, the air permeances and pressure differences required to permit these airflow rates were omitted. The calculations were done using constant inside and outside air temperatures and heat transfer coefficients for vertical surfaces, $+20^\circ\text{C}$ and $15 \text{ W/K}\cdot\text{m}^2$ and -20°C and $7.5 \text{ W/K}\cdot\text{m}^2$, respectively. Horizontal surfaces were assumed adiabatic.

The problem is how the convection through the structure changes the total heat losses. The reference heat losses for a room are the sum of the conductive heat losses and the heat required to warm up the incoming air. If the air infiltrates through the structure, the temperature of the incoming air rises, decreasing the convection heat losses. At the same time the conductive heat losses increase because the temperature gradient increases at the surface. The total heat recovery effect of the structure (Nu^*) in a certain airflow rate can be given as the ratio between the total heat losses of the infiltration case (with heat recovery) and those of the reference case (without heat recovery) with the same airflow rate.

$$Nu^* = \frac{\sum q \text{ (heat recovery)}}{\sum q \text{ (no heat recovery)}} \quad (6)$$

Figure 9 shows how the relative, total heat recovery effect depends on the infiltrating airflow rate and also on the structural thickness according to calculations. The Nusselt number has a minimum value with a certain airflow rate, which depends mostly on the convection route in the structure. This minimum value corresponds to the maximum heat recovery, and the airflow rate of this value can be considered as an optimum value for the structure. If the thickness of the thermal insulation layer increases, then the optimum value of air infiltration rate decreases because the transmission heat losses are smaller with higher thermal resistance and they can be covered with a smaller airflow rate.

Figure 10 shows the temperature distribution with different airflow rates for the uniformly distributed air infiltration. In Figure 10 the inside surfaces are set to be at the same position though the structural thickness coordinate x has zero point at the cold surface. The convective temperature fields are bent so that the temperature gradient increases toward the warm surface. With airflow rates smaller than the optimum value ($0.25 \text{ dm}^3/\text{s}\cdot\text{m}^2$ in Figure 10) the temperature fields and also the incoming air temperatures for different structural thicknesses differ from each other, as expected.

With airflow rates higher than the optimum value ($1.0 \text{ dm}^3/\text{s}\cdot\text{m}^2$) the temperature distribution near the warm surface is almost the same for different structure thicknesses. The inside surface temperature and the temperature of incoming air are almost independent of the insulation thickness. This means that with an airflow rate of $1.0 \text{ dm}^3/\text{s}\cdot\text{m}^2$ through a structure with 200 mm thick thermal insulation, the first 100 mm of the thermal insulation has almost no influence on the thermal behavior of the structure. In this case, the total heat losses through the structures are almost the same (50.0 and $48.9 \text{ W/K}\cdot\text{m}^2$ for 100 and 200 mm insulation thicknesses, with surface temperature values of $+14.3$ and $+14.4^\circ\text{C}$, respectively). This is because the air infiltration now dominates the heat losses, and thus the temperature gradient at the inside surface (control surface for heat losses) is nearly the same for different thicknesses. If the air infiltration rate could be controlled to be on a level that corresponds to the transmission heat losses, the inside surface and air inlet temperatures would be in a correct level.

In the design of dynamic wall structures with uniformly distributed infiltration flow, the inside surface (and incoming air) temperature is the critical parameter that sets the highest possible air infiltration rate. When the maximum air infiltration rate is fixed, the thickness of the thermal insulation has to be chosen according to this value in order to get the optimum heat recovery. With higher airflow rates, the thickness of the optimum thermal insulation becomes smaller. For example, in a 250 m^3 small house, with an 85 m^2 dynamic wall structure, the $0.5 \text{ dm}^3/\text{s}\cdot\text{m}^2$ airflow rate (optimum for insulation thickness about 100 mm and $\Delta T = 40^\circ\text{C}$) corresponds to an air exchange rate of 0.61 per hour.

The results in Figure 9 and 10 are valid for a temperature difference of 40°C over the structure. The optimum value for the infiltrating airflow rate depends on the conductive heat losses in a non-convective case, i.e., on both the thermal resistance and the temperature difference of the structure.

If the warm inside airflows out through the structure, the structure warms up and the conductive heat losses decrease. The heat recovery effect of a structure with air infiltration and exfiltration is almost the same. Air exfiltration is not critical for inside surface temperature, but for the moisture accumulation due to air convection into the structure.

MOISTURE FLOW AND ACCUMULATION DUE TO AIR CONVECTION

In the simulation program TOCC2D, the moisture flow is divided into diffusion and convective mass flows. The diffusive moisture flow includes both pure vapor diffusion and the flow in liquid phase (both mechanisms are measured in the determination of the material property "vapor diffusivity"). The effects of convection on the moisture movement in structures are analyzed numerically in different convection cases, especially in exfiltration flows which may most change the hygrothermal behavior of a building envelope from that of a non-convective case.

In the first case, the hygrothermal performance of a 2.4 m high structure with 200 mm thick mineral fiber thermal insulation (19 kg/m³) covered from the inside with 12 mm wood chip board and from the outside with 12 mm wood fiber board was analyzed (Figure 11). The initial conditions for the structure and surrounding air spaces were +20°C and 1100 Pa vapor pressure. At the moment $t = 0$ the climate conditions of the other air space changed to -20°C and 70 Pa vapor pressure.

Three different cases of convection were analyzed: no airflow in the structure, only natural convection in the thermal insulation, and an exfiltration airflow through the structure, assuming air cracks at the top of the inside board and at the bottom of the outside board. Assuming the same pressure level for inside and outside air spaces at the bottom of the structure, the exfiltration flow rate was 0.034 dm³/s·m², which was caused by the temperature difference between the inside and outside air spaces.

Figure 11 shows the calculated relative humidity fields for all three cases after four to eight days. The moisture distribution is strongly changed from the original values. Because of the high initial moisture value, condensation conditions are reached in every case; without convection in about eight days, with natural convection loop in about six days at the upper part of the outside covering board (also verified with field experiments), and with exfiltration in about four days the condensation area covered half of the insulation thickness at the upper part of the structure. Even natural convection strongly changes the moisture distribution in the area of mineral fiber insulation and air exfiltration caused only by temperature difference can lead to rapid local moisture accumulation.

A more realistic case was simulated with the structure in Figure 12, where the air exfiltrates through the air cracks of the corner area. A schematic airflow field through the structure and the calculated temperature and relative humidity fields are also presented.

The air leakage of the structure was estimated according to field experiments (Kohonen et al. 1986). Although there was constant air exhaust from the test building, the wind and temperature differences caused such a pressure field that in some parts of the building envelope (for example, in wall and ceiling joints) the inside pressure was higher than that of the outside air in that level. This led to air exfiltration through that part of the building envelope.

A three-week period with air exfiltration was selected from the weather data for the numerical simulation. The outside temperatures varied from -10°C to -29°C and the air exfiltration rate varied from 0.05 to 0.12 dm³/s·m (volume flow per crack width) during the simulation period. The indoor climate conditions were kept constant during the simulation (+20°C, 1200 Pa).

Figure 12 shows the calculated temperature and relative humidity fields after the three-week exfiltration period. The condensation area is spread widely near the inside opening and also throughout the inside surface of the outer wood fiber board. With a mean airflow rate 0.08

$\text{dm}^3/\text{s}\cdot\text{m}$, the daily moisture accumulation by convection was about 50 g. Figure 13 illustrates the change of the moisture content field in the wood framing of the structure in Figure 12 during the three-week period of air exfiltration.

According to the calculations, air exfiltration through a lightweight structure may lead to local critical moisture conditions during a few weeks, especially if there are no infiltration periods, which could dry out the structure.

CONCLUSIONS

Structural airtightness is one of the main parameters that influences the hygrothermal behavior of the building envelope. Usually an ideal structure that has no air leakage routes in material boundaries works hygrothermally as planned. Air cracks and other non-idealities may increase airflow locally so that the temperature and moisture fields can get critical values.

Forced convection caused by wind pressure may considerably increase the heat losses, especially in structural joints such as corners, where there are also structural thermal bridges (for example, wood framing). The wood framing may also work as a convection obstruction by changing the direction of airflow and reducing the airflow velocity, which can prevent the local surface temperatures from decreasing to critical values.

Air infiltration and exfiltration through the building envelope causes heat recovery from transmission heat losses. The total heat recovery effect considering the heat balance of the room air (with increased conduction and reduced infiltration heat losses) can be more than 20%, in the case of uniformly distributed air infiltration through the thermal insulation of the structure. The total heat recovery effect depends on the conductive heat losses of the structure and on the airflow path, and it will get a maximum value with a certain airflow rate, which is typical for the case (structure and boundary conditions).

Long-time inside airflow through a structure may cause severe moisture damage especially during a heating period, when the incoming air has a high partial vapor pressure value compared to the saturation vapor pressure value at the inside layers of the structure. This leads to moisture condensation in the building envelope. Limits for critical exfiltration rates should be analyzed case by case because they depend on both the hygrothermal properties of the structure and on the inside air and climate conditions.

To ensure correct hygrothermal behavior of the building envelope, strong air pressure gradients in thermal insulation and long-time air exfiltration should be avoided. This requires the controlling of air pressure levels at the building envelope and air spaces (for example, by structural means), keeping the pressure gradients in air gaps low and the structures airtight, or planning the infiltration/exfiltration flow routes to correspond to the local air pressure levels and airflow rates.

NOMENCLATURE

| | | |
|-------------|---|--|
| c_p | = | specific heat capacity, $\text{J}/\text{kg}\cdot\text{K}$ |
| d | = | thickness (of thermal insulation), m |
| g | = | gravitational pull, $= 9.81 \text{ m}^2/\text{s}$ |
| h | = | height, m |
| K_v | = | permeability, m^2 |
| p | = | air pressure, Pa |
| p_v | = | partial vapor pressure, Pa |
| Ra^* | = | modified Rayleigh number (Equation 5) |
| q | = | heat flux, W/m^2 |
| T | = | temperature, K or $^{\circ}\text{C}$ |
| v | = | airflow velocity, m/s |
| \dot{V}'' | = | airflow rate per structure area, $\text{dm}^3/\text{s}\cdot\text{m}^2$ |
| x | = | horizontal coordinate |
| y | = | vertical coordinate |

α = convective heat transfer coefficient, W/K·m²
 β = volumetric expansion coefficient for air, =1/T, 1/K
· = thermal conductivity, W/K·m
 ν = kinematic viscosity, m²/s
= density, kg/m³

REFERENCES

Kohonen, R.; Kokko, E.; Ojanen, T.; and Virtanen, M. 1985. "Thermal effects of air flows in building structures". Technical Research Centre of Finland, research report 367, p. 81.

Kohonen, R., et al. 1986. "Natural and forced convection in mineral fiber wall insulation". Technical Research Centre of Finland, research report 431. p. 119.

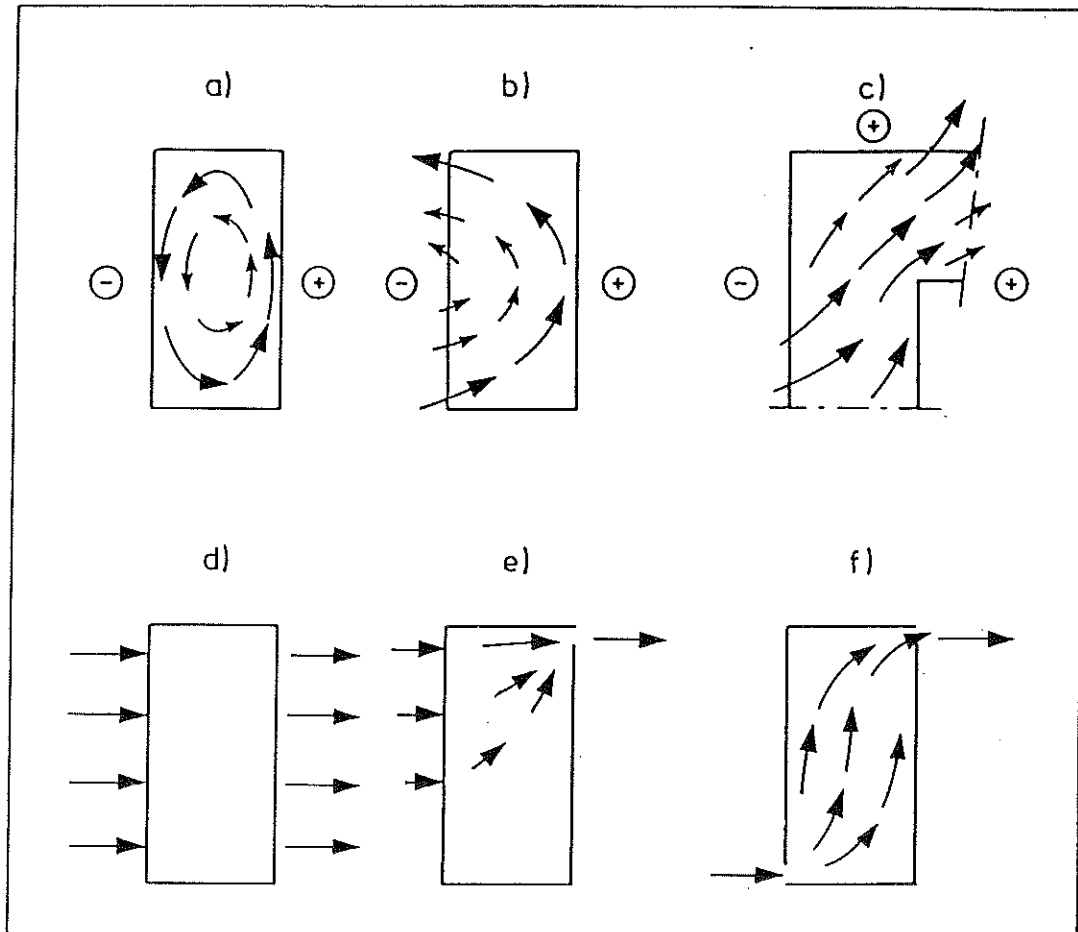


Figure 1. Typical cases of air convection in building envelope: natural convection (a and b); forced convection (c); air in/exfiltration (d through f)

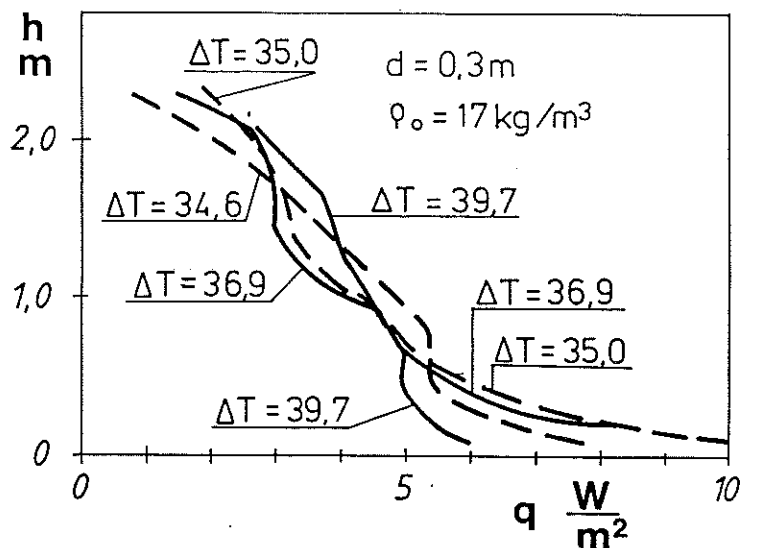
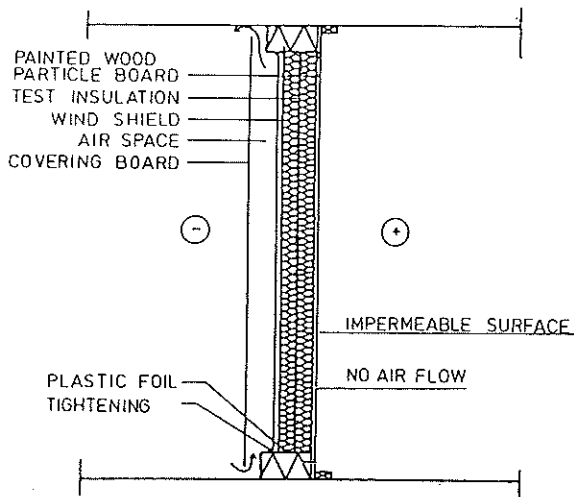


Figure 2. Test setup of laboratory measurements on thermal effects of natural convection and measured heat flux distribution for closed and semi-open structures

— closed structure
 - - - no wind barrier

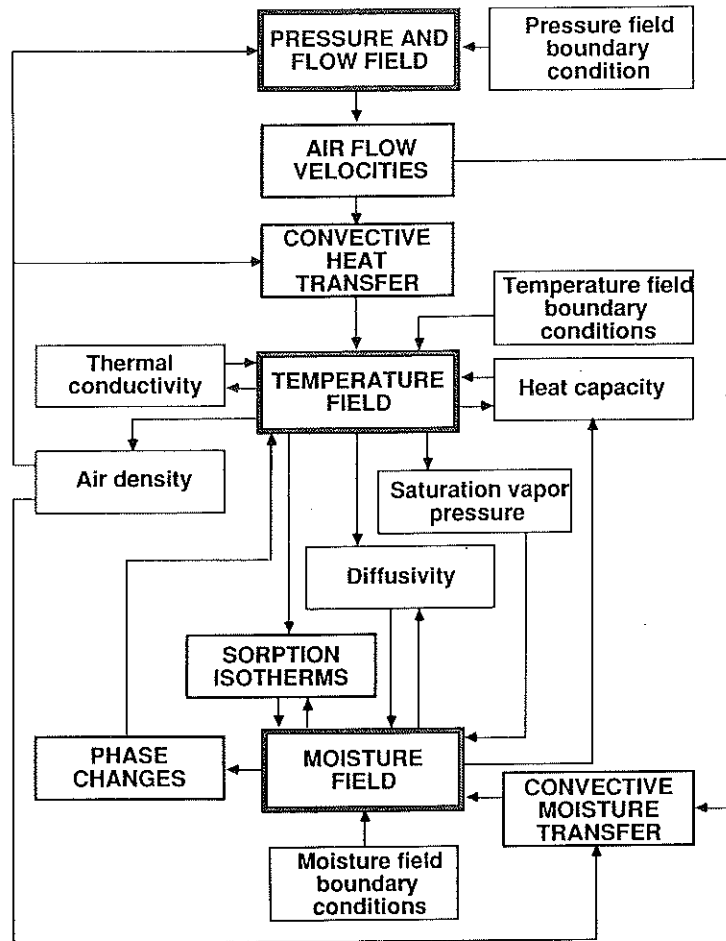


Figure 3. Flow chart of TCCC2D for the solution of air flow, temperature and moisture fields

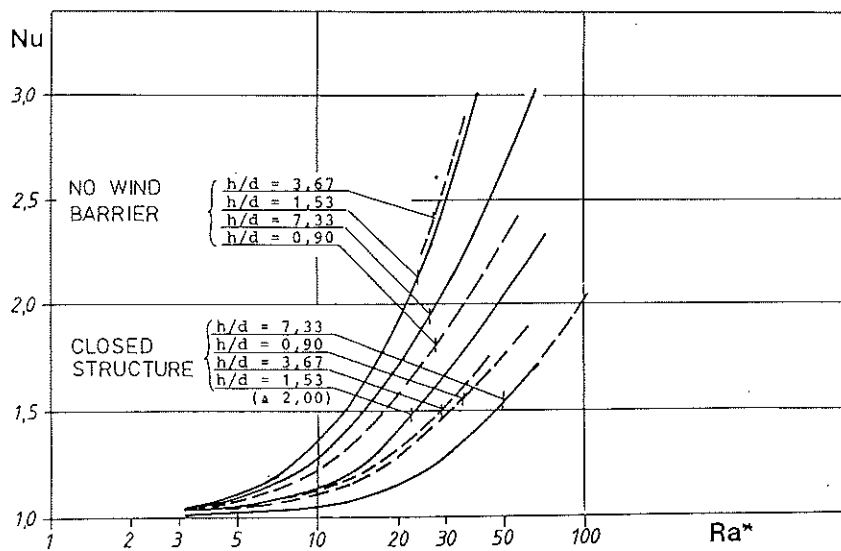


Figure 4. The calculated Nusselt numbers for ideal closed and semi-open structures as a function of the Rayleigh number. Aspect ratio h/d is a parameter.

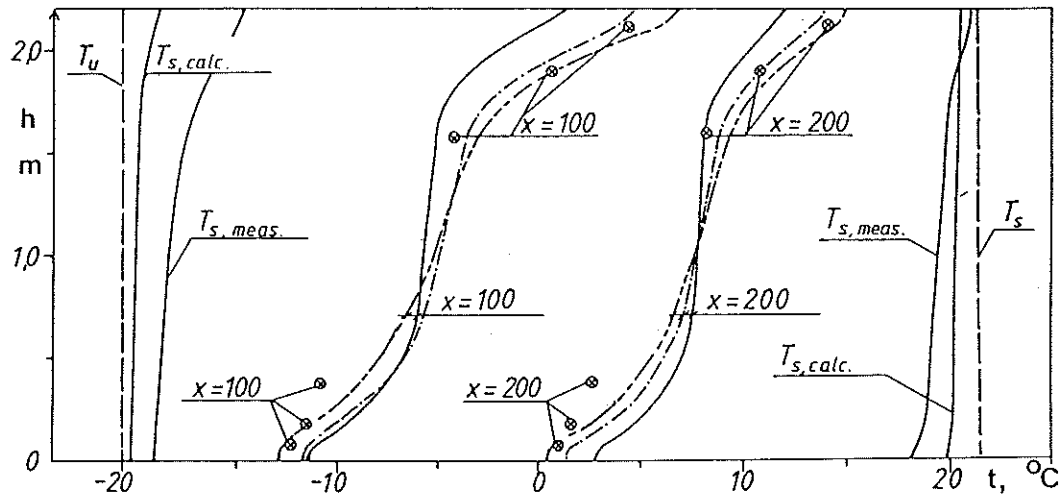


Figure 5. Measured and calculated temperature values for a structure without wind barrier with $\Delta T = 40^\circ\text{C}$ (Pure natural convection)

\circ measured values
 — calculated for ideal structure
 - - - calculated for a structure with small air leakage at inside vertical boundaries of mineral fiber thermal insulation

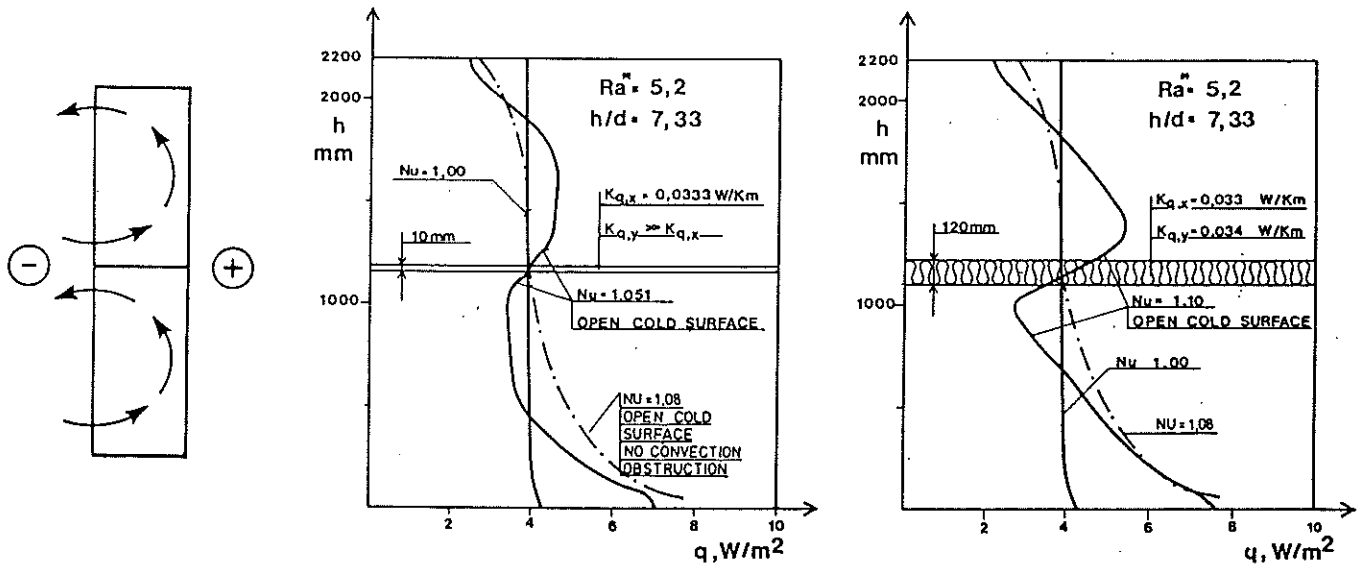


Figure 6. Calculated heat flux distribution for semi-open structures with horizontal convection obstruction. The convection obstruction has no thermal resistance (left) and has a great thermal resistance (right).

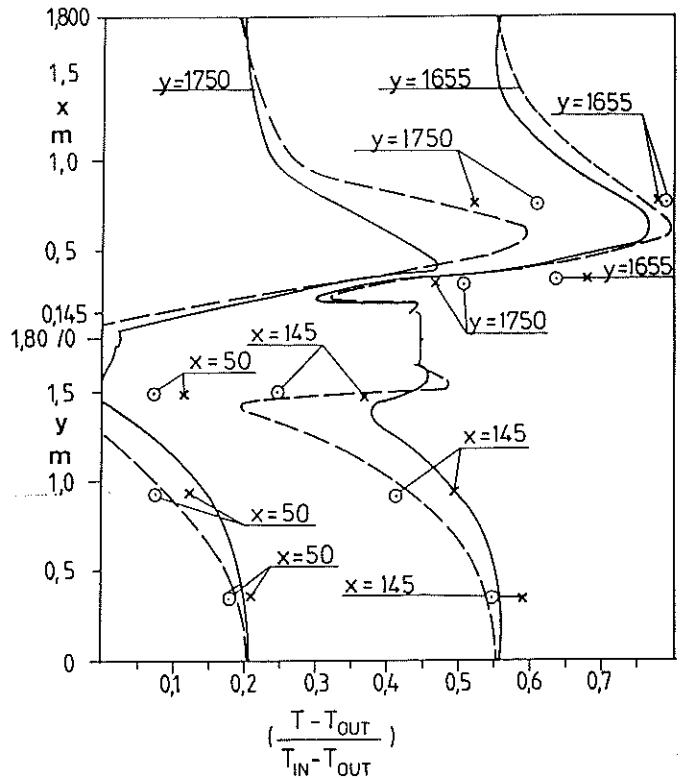
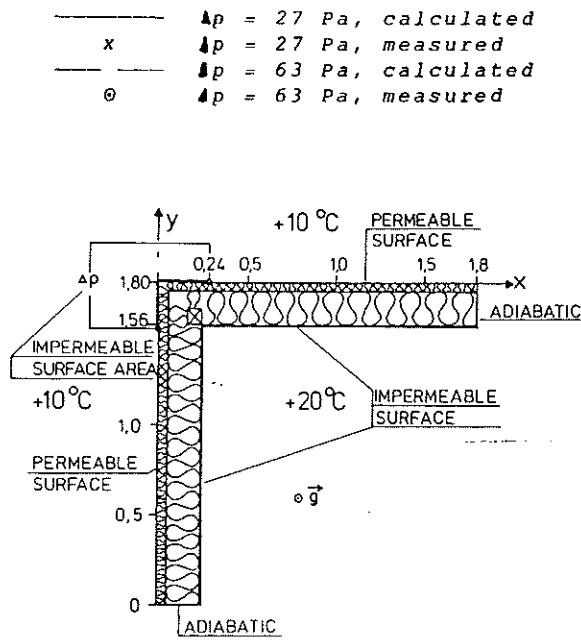


Figure 7. Forced convection in a corner structure. Measured and calculated relative temperature values with 27 Pa and 63 Pa pressure differences over the corner

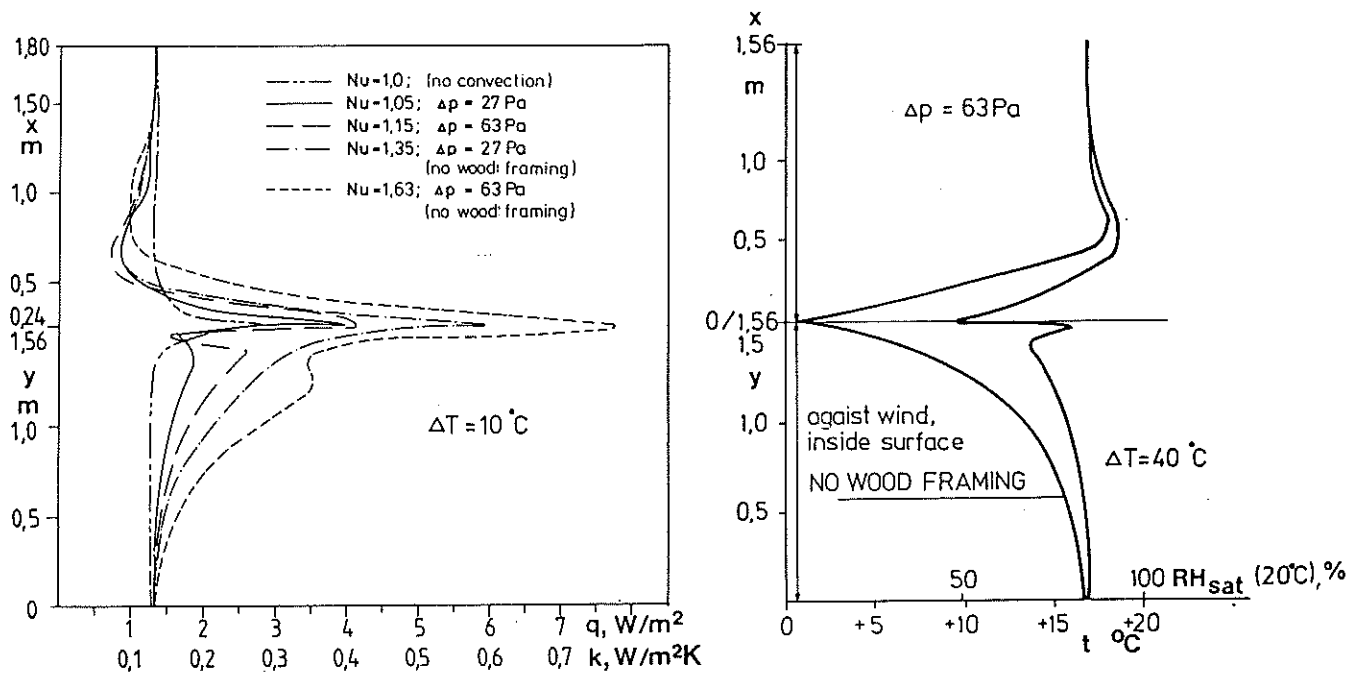


Figure 8. Calculated heat flux distribution for the structure in Fig. 7 with $\Delta T = 10^\circ\text{C}$ temperature difference with and without wood framing in the corner (left) and calculated inside surface temperatures for the same structure (right) with $\Delta T = 40^\circ\text{C}$ and $\Delta p = 63 \text{ Pa}$.

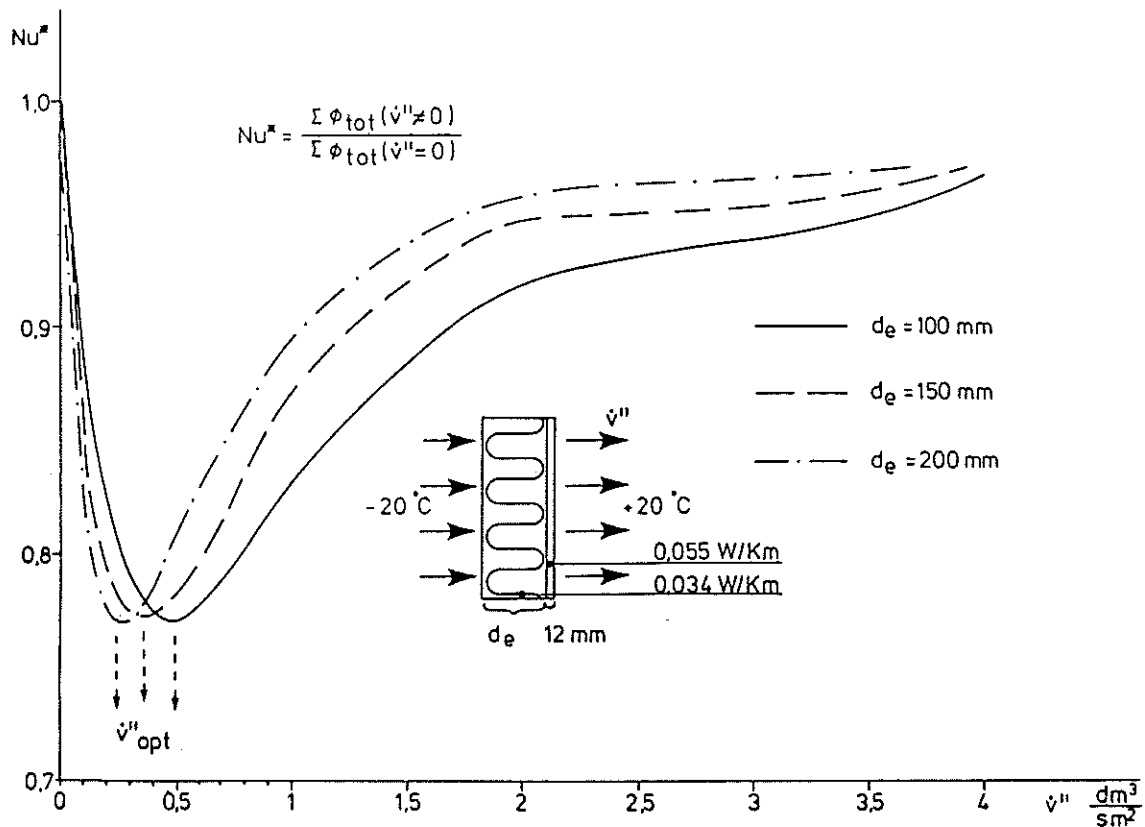


Figure 9. Relative total heat recovery effect for a dynamic wall structure with uniformly distributed infiltration air flow for different thicknesses of the thermal insulation with $\Delta T = 40 \text{ }^\circ\text{C}$

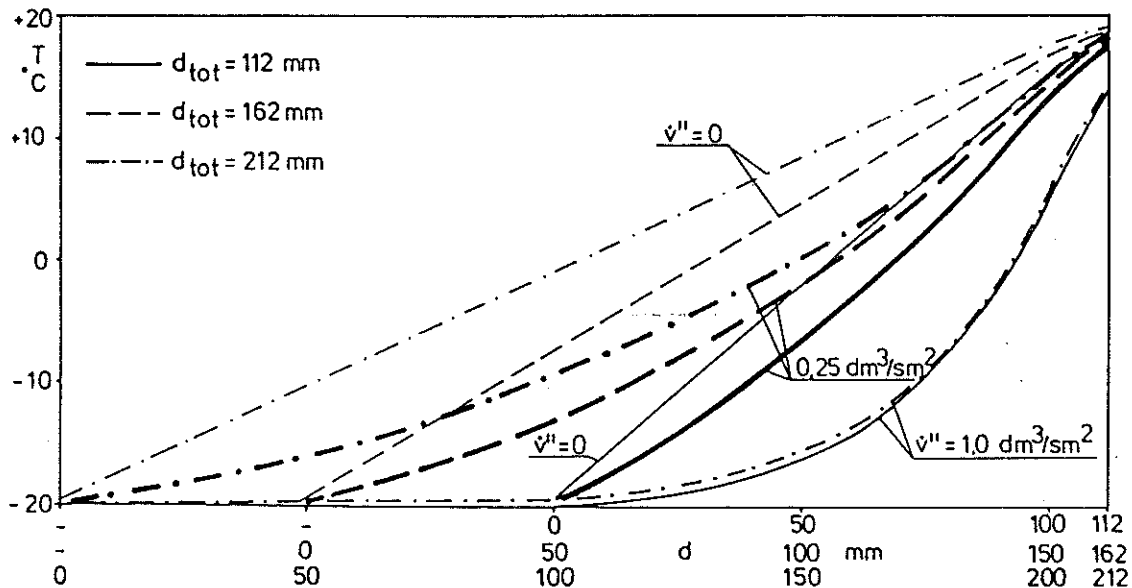


Figure 10. Calculated temperature distribution in the thermal insulation of an air infiltration case. When $\dot{V}'' > \dot{V}''_{opt}$ (Fig 9), the heat flux has almost no dependence on the insulation thickness.

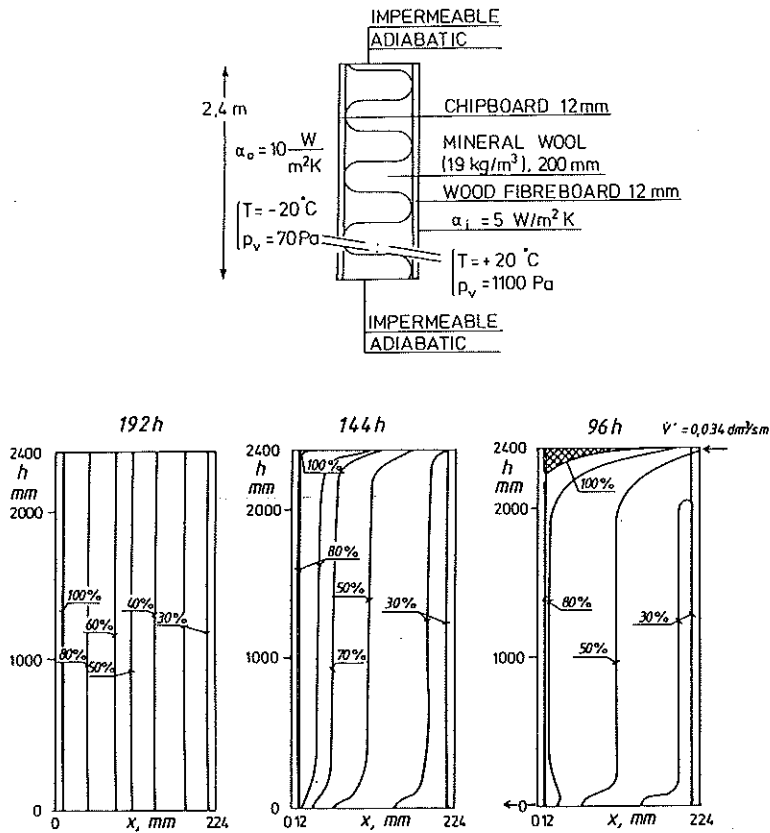


Figure 11. Analyzed structure and boundary conditions (upper Fig.) and relative humidity fields for cases with no convection (left), closed structure with natural convection (in the middle) and air exfiltration (right) after 4 to 8 days from the beginning of the calculation

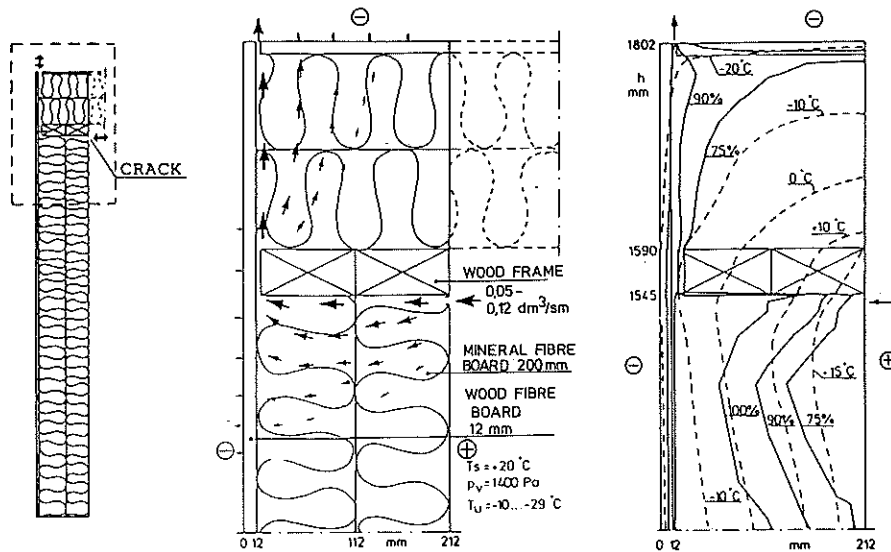


Figure 12. A structural corner with air exfiltration. Air flow rates and outside air conditions are chosen from measured values in field experiments. Air flow field, temperature and relative humidity fields after 3 weeks exfiltration with air flow rate varying from 0.04 to 0.12 dm³/s·m and outside air temperature from -10 to -29°C.

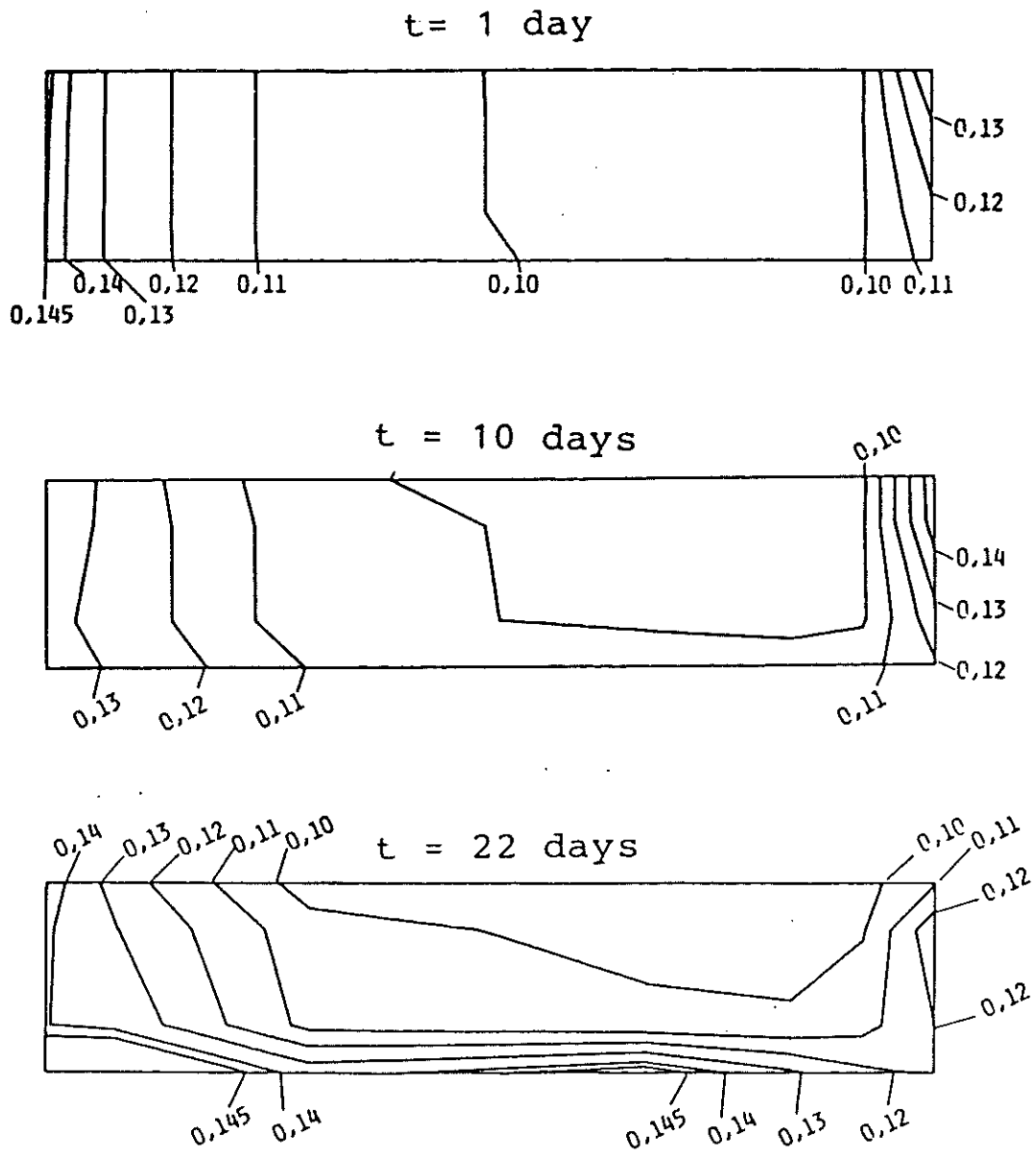


Figure 13. The calculated change of moisture content (kg/kg) fields in wood framing of the structure in Fig. 12 in the case of air exfiltration for a 22-day-period. Initial moisture content was 0.10 kg/kg.